

How can the green sulfur bacteria use quantum computing for light harvesting?

D Drakova¹ and G Doyen²

¹ State University of Sofia, Faculty of Chemistry, Sofia, Bulgaria

² Ludwig-Maximilians-University, Munich, Germany

Abstract

Long lasting coherence in photosynthetic pigment-protein complexes has been observed even at physiological temperatures (1; 2; 3). Experiments have demonstrated quantum coherent behaviour in the long-time operation of the D-Wave quantum computer as well (4; 5). Quantum coherence is the common feature between the two phenomena. However, the 'decoherence time' of a single flux qubit, the component of the D-Wave quantum computer, is reported to be on the order of nanoseconds, which is comparable to the time for a single operation and much shorter than the time required to carry out a computation on the order of seconds. An explanations for the factor of 10^8 discrepancy between the single flux qubit coherence time and the long-time quantum behaviour of an array of thousand flux qubits was suggested within a theory where the flux qubits are coupled to an environment of particles called gravonons of high density of states (6; 7). The coherent evolution is in high dimensional spacetime and can be understood as a solution of Schrödinger's time-dependent equation.

Explanations for the quantum beats observed in 2D Fourier transform electronic spectroscopy of the Fenna-Matthews-Olson (FMO) protein complex in the green sulfur bacteria are presently sought in constructing transport theories based on quantum master equations where 'good' molecular vibrations ('coloured noise') in the chlorophyll and the surrounding protein scaffold knock the exciton oscillations back into coherence (8; 9). These 'good' vibrations are claimed to have developed in three billion years of natural selection. These theories, however, face the discomfoting experimental observation that "attempts to scramble vibrational modes or to shift resonances with isotopic substitution miserably failed to affect the beating signals" (10). As a possible way out of this dilemma we adopted the formalism of the quantum computation to the quantum beats in the FMO protein complex.

Keywords: long-living coherence, quantum biology, green sulfur bacteria, emergent quantum mechanics

1 Introduction

When in 2007 the New York Times published an article suggesting that plants were quantum computers, quantum information scientists exploded into laughter (11). Their concern was, of course, decoherence which is believed to be one of the fastest and most efficient processes in nature. The laughter is over and quantum biology is firmly established, but the mechanism

which sets decoherence apart is still under debate.

The experiments by Engel et al. show that long lasting coherence in photosynthetic pigment-protein complexes is observed at physiological temperatures (1; 2; 3). Quantum coherence over hundreds of femtoseconds in the initial steps of photosynthesis, the transfer of light quanta towards the reaction centers, in green and purple bacteria (12; 13) at room temperature (14; 15), algae at ambient temperature of 294 K (16) and even in living cells of purple bacterium (17; 18) warrant the high efficiency of the light-harvesting process. It has even been suggested that the high efficiency of photosynthesis may be associated with coherent energy and charge transfer on a long timescale (19; 20; 21).

Citing Hildner et al.: "...quantum coherence is the central aspect connecting fields as diverse as quantum computing and light-harvesting" (22).

In 2011 the first commercially available quantum computer was presented by the company D-Wave consisting of an array of more than thousand flux qubits (June, 2015), which solves optimization problems with many free parameters (4; 5). It works as a quantum computer of the quantum annealing type for minutes and even for half an hour. However, a single flux qubit in a Ramsey interference experiment shows coherent oscillations between the two supercurrents for time of the order of 20 ns, which is 8 orders of magnitude shorter than the coherence time of the D-Wave computer (23). The amplitude of the oscillations decays to $1/e$ after 20-25 ns. It is often said that the flux qubit loses coherence within 20 ns, or it dephases, or it is decohered, or it is driven by noise or experimental imperfections. The experimental observation is that the probability for the oscillatory state change decreases exponentially, achieving some non-zero final value, which does not change with time any more.

This was a noteworthy result as a flux qubit is a macroscopic device with dimensions of the order of 10^4 Å. But not less noteworthy was the experimental observation of a coherent quantum behaviour of the Fenna-Matthews-Olson pigment-protein complex not only at low temperature but even at 277 K and the coherent behaviour of the light harvesting complex in the purple bacterium living cell in a dense, wet noisy environment (17; 18). The 'time of coherent development' of the FMO-complex is picoseconds, i.e. 4 orders of magnitude shorter than that of a single flux qubit. With the help of 2D Fourier transform electronic spectroscopy (24)-(27) the amplitude of a photon echo signal as a function of the waiting time between the first two laser pulses, which excite the FMO electronically, and the third laser pulse, which stimulates the photon emission from the exciton, shows beats. The beats, the oscillations in the time development of the photon echo signal, are due to the coherent superposition of two lowest energy excitons shared by all chlorophyll molecules and indicate coherent time development of the FMO-complex during the waiting time. In contrast to the experimental observation, an exponential decay of the photon signal with time would be expected, if decoherence due to interaction with the noisy environment (phonons) of the FMO-complex were effective, as it is generally believed that electronic coherence decays on 10-100 fs timescales (28; 29).

Why is the beating between exciton states observed for picoseconds instead of a fast expo-

nentially decaying signal without oscillations, as decoherence theory suggests? Why is no decay to zero amplitude of the photon signal observed, if decoherence due to interaction with the noisy environment (phonons) of the FMO-complex were effective? The expected question is: why does decoherence not take over and reduce the photon signal of the FMO complex, which is in an environment of many degrees of freedom at high temperature? Decoherence theory aims to calculate the time development of the reduced density matrix of a subsystem and thereby tries to demonstrate that the reduced density matrix very rapidly approaches a quasi-diagonal form. The diagonal matrix elements are then interpreted as probabilities of finding the subsystem in the respective state. Calculations for realistic models are scarce. Notable are those by Joos and Zeh (30), Zurek (31) and, applying to the present investigation, by Lloyd et al. (32).

In contrast to expectations based on the decoherence concept, both the molecular system FMO and the macroscopic flux qubit show long time coherence. The major question is: Why does decoherence in both cases play no role? The damping of the Ramsey fringes in the experiment with the single flux qubit cannot be due to decoherence, because otherwise the D-Wave quantum computer, with an array of 1000 flux qubits, would not be able to function as a quantum computer for minutes.

Semi-classical diffusive models based on stochastic dynamics have been extensively applied to study energy and charge transport in biological systems (33; 34; 35). Within a quantum master equation approach the time development of the reduced density matrix is evaluated (32), the effect of the phonon environment is simulated by an additive Redfield term, which is dropped for the study of the time development. With a very special selection of the phonon environment (coloured noise) the beats of the photon amplitude are reproduced, but the finite final value of the photon amplitude is not explained. Furthermore the 2D Fourier transform experiment shows that no special phonons are involved in the damping of the signal, changing the FMO phonon spectrum does not influence the results (10).

Theoretical attempts based on the electron incoherent hopping process (33; 36) between pigment molecules in the photosynthetic unit have been suggested (37).

A discussion topic is the nature of the superimposed coherent states in the protein-pigment complexes. Vibrational, electronic or vibronic states may be involved, with indications from experiment favouring their vibronic character ((13), (38)-(44)).

We focus on the experimental observation in the 2D Fourier transform electronic spectroscopy which demonstrates coherence by the Fenna-Matthews-Olson protein-chlorophyll complex of green sulfur bacteria over times longer than 1000 fs and even at high temperature (277 K). The amplitude of the measured photon echo signal oscillates with time, which is an indication of coherent behaviour, suggested as the basis for the extreme efficiency of the photon transfer towards the reaction center and hence of the photosynthetic processes in the depth of the Black sea. The expectation that decoherence due to the chaotic molecular environment, considered to be very fast, on the timescale of $10^{-20} - 10^{-17}$ s, in the bacterium cell at physiological

temperatures will destroy coherence, is not confirmed experimentally. The issues we will address in the present article refer to:

- Why is decoherence not effective and not fast enough to destroy coherence?
- Despite that the photon amplitude beats are exponentially damped with time, the final value is finite, larger than zero even at high temperature. What is the reason for this?
- Missing isotope effect, random exchanges of ^1H atoms or of ^{12}C with their isotopes do not change the picture. Random hydrogen exchange with deuterium and exchange of all ^{12}C with ^{13}C or even the whole hydrocarbon side chain of the pigment by a different one do not affect the coherent behaviour (45). This procedure certainly changes the phonon spectrum, but the results on the coherent quantum beats are not influenced. Coherence is experimentally shown in bacteria (1; 2; 12; 15; 17; 18), algae (16) and green plants (46). The structure of their protein backbones differ and hence the protein scaffolds cannot serve as the ubiquitous protection of electronic coherence, as it is suggested in refs. (1; 2; 12; 16).
- A discussion issue is the nature of the coherent states and the role of the environment. Our results are in favour of vibronic states, many-particle states involving electron exciton components and local vibrations of the protein backbone.

The dying out of the oscillations between the two supercurrents in the single flux qubit was explained in a coherent picture solving Shrödinger's time dependent equation in high dimensional spacetime (7). The decisive features of the theory are summarized in the next section together with the description of a simple model of the physical picture of the processes in FMO 2D Fourier transform electronic spectroscopy. The results are presented in section 4, followed by a summary and conclusions.

2 The model and the physical picture

The FMO protein complex consists of seven chlorophyll molecules in a protein cavity. There is an eighth bacteriochlorophyll molecule outside the cavity whose interaction with the rest seven molecules can be neglected. The first two laser pulses in the 2D spectroscopic experiment, delayed by only 20 fs from each other, excite two excitons and lead to their coherent superposition, which results in the beating signal. The time between the first two laser pulses, i.e. the coherence time τ , in different 2D spectroscopic experiments is of the order of 20 to 500 fs and the duration of each pulse is 15-40 fs. These times are very short compared to the time needed to establish the entanglement with the gravonons (representing local version of the gravitons), the environmental excitations we take into account in addition to the excitations considered in other theories like phonons and electron-hole pairs. Therefore for the purposes of our theory the first two laser pulses are regarded as one double pulse. The third laser pulse is applied after a waiting time varying from 0 fs to 1000-1500 fs and serves to stimulate the

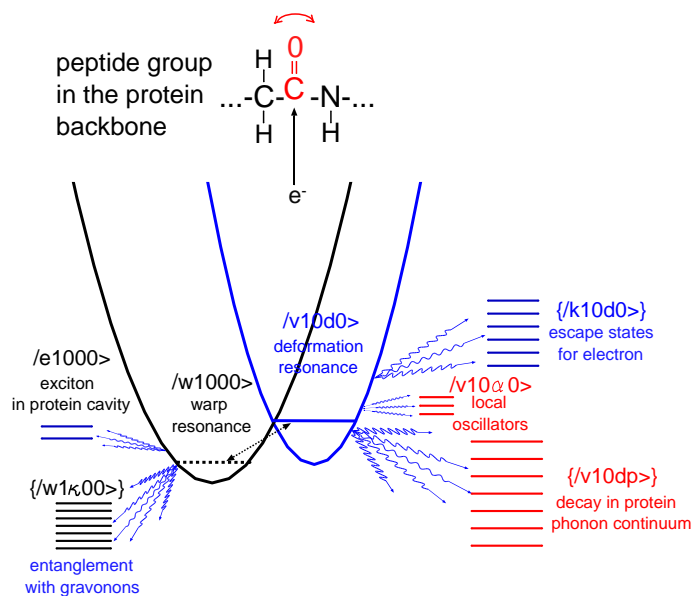


Figure 1: Model for studying the quantum coherent behaviour of a complex of bacteriochlorophylls (FMO complex) in a protein scaffold in the green sulfur bacteria. The protein scaffold provides the carbon atom in the carbonyl CO fragment to capture the nucleophile, the exciton electron, in a transient negative ion resonance which relaxes and couples with phonon modes in the protein and excites local rocking and wagging motion of the carbonyl CO fragment. The entanglement with gravonons is effective within the NIR, but as it develops slowly compared to the coupling with the phonons, its effect during the tiny burst, induced by the double laser pulse, is neglected in the calculations. In this schematic drawing the gravonon spectrum is plotted on a scale magnified by a factor 10^8 and differs from the scale of the other spectra.

emission of the photon, which is recorded as the photon echo after the rephasing time t .

The physical picture we describe is the following. The exciton electron wave packet is diffuse, penetrating in the protein scaffold, where as a nucleophile in a nucleophilic-like reaction the exciton electron attacks the positively polarized carbon atom of the carbonyl CO fragment. The electron can be transiently accommodated in the $3s$ -affinity like orbital on the carbonyl carbon atom creating a transient negative ion resonance (NIR). Thus the electron penetrates in the carbon core region where it interacts gravitationally with the atom core. At interatomic distances the strength of the gravitational interaction is enhanced by many orders of magnitude, if hidden extra dimensions exist. In the spirit of Einstein's general relativity the gravitational interaction between masses deforms spacetime and we introduce a basis state called warp resonance for the electron (fig. 1), where it entangles with the gravitons (the messenger particles of the gravitational field). Locally a soft gravonon structure is generated, which is constructed as a correlated motion of 3-4 atoms leading to the warping. The soft gravonons in our theory are the solution of interacting quantum harmonic oscillators centered on the 3-4 atoms close to the NIR. For more details on the theory concerning the generation of the gravonons see refs. (7; 47).

The electromagnetic field acts as an external force on the carbon atom and, together with the thermal fluctuations, shifts it slightly in a different position creating a local deformation in the protein chain. This is no wonder since the local vibrations of the atoms in the carbonyl CO fragment are different if the carbon atom has captured transiently the electron or not. The local deformation of the protein chain occurs around the NIR, it is associated with slight increase in energy, and is described by introducing a basis state called deformation resonance for the core motion of the carbonyl fragment. Furthermore excitation of vibrational modes like the rocking and wagging motion of the carbonyl CO fragment is possible which we describe by coupling the deformation resonance to two local harmonic oscillators, i.e. to local vibrational modes (fig. 1).

In the deformation resonance coupling to the extended phonons of the protein backbone is also effective, leading to phonon excitation and energy dissipation from the local region (fig. 1). The exciton electron has the option to decay from its localized state in the NIR in delocalized electron states, called 'escape states' because total energy has to be conserved, if phonons are excited. Electron states delocalized over the chlorophyll assembly with the $3s$ -affinity like orbital of the carbonyl carbon atom as component play this role. It is within the deformation resonance that coupling with the phonons of the protein backbone is taken into account and energy dissipation from the local region in the protein backbone via phonon excitation may occur. However, due to the interaction between the deformation resonance and the local rocking and wagging modes of the carbonyl CO fragment, reflection to and fro between the local states occurs. Therefore, despite the dissipation into the protein backbone phonons, there remains a local non-zero electron component in the total wave packet, which explains the finite non-zero value of the photon signal in the 2D spectroscopic experiment when the deexcitation of the exciton electron is stimulated by the third laser pulse.

The gravitational interaction of the exciton electron with the carbon atom core has to be in high spacetime dimensions ($11D$) as string theory assumes. Only then gravity is strong enough at small distances and decays fast with distance (r^{-8} power law and nearly 33 orders of magnitude higher value of the gravitational constant in $11D$). The additional 7 spacial dimensions are compactified and are hidden, so that there is no discrepancy with Newton's gravitational law at distances where it was proved valid. Within the warped space the time development of the entanglement of the electron with gravonons leads to the beables.

Beables are mathematically precisely defined as a set of configurations in the expansion of the wave function containing a localized matter field and excited local gravonons. Loosely speaking beables are matter fields (e.g. atoms or electrons) in $3D$ space, entangled with gravonons, which interact with other atoms gravitationally and generate the gravonon structure in high dimensional spacetime. Therefore localized atoms, molecules or electrons in $3D$ space entangled with gravonons in high dimensions in the form of beables exist as long as the beables and the entanglement with the gravonons exist.

The word "beable" has been coined by John Bell (48) as a terminology against the word observable: "The concept of 'observable' lends itself to very precise mathematics when identified with 'self-adjointed operator'. But physically, it is a rather wooly concept. It is not easy to identify precisely which physical processes are to be given the status of 'observations' and which are to be relegated to the limbo between one observation and another."

We use the expression beable in the sense of John Bell's *local* beable. According to our proposal signals in experiments in $3D$ space can be received only via beables and hence measurements are tied to beables (47). Expressed with John Bell's words: "One of the apparent non-localities of quantum mechanics is the instantaneous, over all space, 'collapse of the wave function' on 'measurement'. But this does not bother us if we do not grant beable status to the wave function."

Already in 1927 it was revealed that an interference pattern shows up on a photographic plate only when the number of photons falling on the plate is very large (49). The history of photon detection is nicely reviewed in ref. (50). Here the results of Dempster and Batho are summarized in such a way that when, during the so called 'collapse of the wave function', the photon is destroyed, there appears somewhere on the photographic plate an atom of elemental silver which will act as an embryo from which, by photographic development, a small seed of silver will grow. The silver embryo is much smaller than the electromagnetic wavelength and constitutes the beable in our picture.

Applied to the spectroscopic method used in the bacteria experiment investigated here this means that the photon of the laser pulse occupies during the interference process at least the whole volume of the cavity embraced by the protein scaffold, but if the photon is measured and hence destroyed, there appears a beable (embryo) formed in the detection devices of the experimenters.

The described mechanism of the so called collapse of the wave function has by now also been established for matter fields (51)-(53). For an electron in an excitonic state of the chlorophyll it means that the wave function of this electron occupies during the interference process the whole volume of the chlorophyll, but when it hits the protein scaffold, which acts as a kind of screen, the electron becomes localized in a tiny volume of the size of the silver embryo, this being the carbon affinity level of the carbonyl group in the model developed here.

Before the laser pulse is sent in, the electron will be almost with certainty in such a beable. The laser pulse initiates then an interference process where the many particle wave function describing photon, electron, phonon etc. extends over the whole volume embraced by the protein scaffold. This many particle wave function is not a beable, but, in John Bell's terminology, rather a 'limbo state'. As time passes on a matter field will somewhere entangle with gravonons and form a beable which destroys the photon. If beforehand the photon 'localizes' in a beable in the detection devices of the experimenters, it will do so proportional to the light intensity in the system.

2.1 Chooser mechanism, beables created with the chooser mechanism

The question is why does the exciton electron become localized on a single carbonyl carbon atom of a single carbonyl CO fragment in the protein backbone? Quantum particles, e.g. the exciton electron, may become localized via the entanglement with gravonons in the form of beables. However, as the gravitational interaction even in high dimensional spacetime is weak, entanglement with gravonons can be effective on the energy shell alone. In the present model the exciton electron is localized because via the entanglement to gravonons a beable is generated by the local and strongly distant dependent interaction with the gravonons. In the case of on-shell coupling even a very weak coupling with the gravonons is effective. Just a few or a single carbonyl carbon atom in the protein chain provide the condition for on-shell coupling with the initial exciton electron wave packet. This is the chooser mechanism for the site of most favourable entanglement with gravonons. The chooser mechanism is responsible for the appearance of stuck particles on single sites on the detection screen in double slit experiments (54).

The exciton is a diffuse object. Its overlap with all carbonyl CO fragments in the protein backbone would mean that the electron might be thought to reside on all carbonyl carbon atoms in CO sites at the same time and would couple to all degrees of freedom all over the protein chain. Then decay in the environmental degrees of freedom resembles decoherence and is commonly predicted to be very fast. This is, however, not the case in our theory because the chooser mechanism selects a single carbonyl carbon atom on a single CO site where the condition for degeneracy coupling with the gravonons is fulfilled, i.e. where the chooser mechanism leading to the transient localization of the electron works. The electron can go to only a single carbonyl carbon atom in a single CO site, chosen by the degeneracy coupling criterion.

Beables are destroyed when the entanglement with the gravonons is changed or truncated.

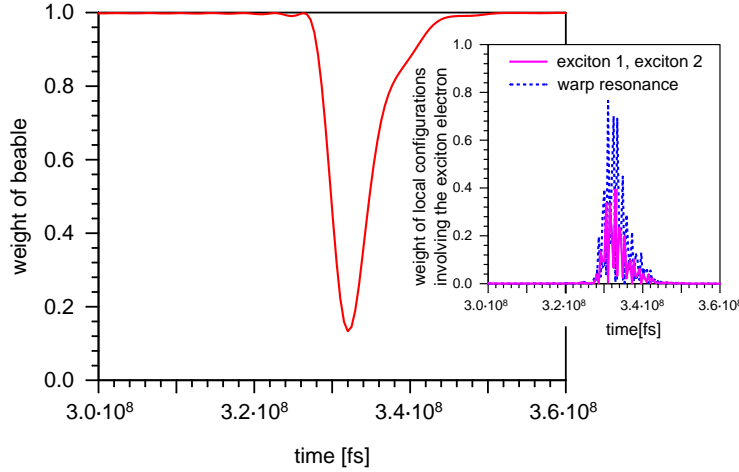


Figure 2: Time development of the entanglement of a quantum particle, e.g. the exciton electron, with the gravonons, generating the beable. Within the beable the electron is localized in the warp resonance and can interact with the photon field, i.e. it can be measured. As soon as the lifetime of the gravonons in the high hidden dimensions expires, the electron bursts out of the entanglement with the gravonons and is released in $3D$ space. This is the tiny burst in the figure. It exists for a short time before the entanglement with the gravonons is reestablished, which takes $5 \cdot 10^{-9} - 10^{-8}$ s. The inset shows the bursting of the exciton electron out of the beable in three dimensional space (in the warp resonance and the excitons in the cavity) during the tiny burst.

This occurs as a tiny burst in the time development of the beable caused for instance by the laser pulses (fig. 2). In the tiny burst the quantum particles (atoms, molecules, electrons) are released from the entanglement with the gravonons and they burst out of the beable into $3D$ space in a 'limbo state'. All states where particles are not entangled to gravonons we call limbo states.

Within the beable the electron is localized in the warp resonance and can be measured. As the lifetime of the gravonons in the high hidden dimensions expires, the entanglement of the localized electron with the gravonons is truncated and the electron is released in $3D$ space. The electron bursts out of the entanglement with the gravonons.

To demonstrate the destruction and re-creation of the beable the Hamiltonian, described in section 3, is diagonalized without the term $H_{el-grav}$. Then this term is transformed to the new diagonalized basis and the time dependent Schrödinger equation (TDSE) is solved as described in section 3. The tiny burst can be seen in fig. 2. It exists for a short time before the entanglement with the gravonons is reestablished which takes $5 \cdot 10^{-9} - 10^{-8}$ s. Within the tiny burst experimentally nothing can be recorded about the electron. This situation does exist in different experiments: in double slit diffraction experiments with electrons and molecular beams we know nothing about the quantum particles during their time of flight between the

source and the detection screen; in laser-induced desorption we know nothing about the adsorbate for the time of flight between the state with the adsorbate as a beable on the substrate surface and in the mass spectrometer, where a new beable is created.

The effect of the double laser pulse in experiment is to induce a tiny burst in the time development since the laser pulse creates an electromagnetic field, which exerts a force on the localized particle within a beable. Slight shifts of the atom positions mean changed local gravonon structure and destroyed coupling to the gravonons (very short ranged), hence the beable is destroyed. For instance, the double laser pulse in the 2D spectroscopic experiment interacting with the electric dipole due to the localized electron on the carbon atom, induces a slight shift of the carbon atom and rocking and wagging motion of the carbonyl CO^- fragment in the protein. This would cause such a drastical change in the gravonon structure, typical for the beable configuration existing before the laser induced tiny burst, that the entanglement with the gravonons is destroyed. This is how the gravonon structure and the beable are destroyed by the laser pulses. As the entanglement with the gravonons develops in a period of time of the order of 10^{-8} s, in the laser-pulse-induced tiny burst the electron is released from the entanglement with the gravonons, however, its coupling with other excitations, living in 4 dimensional spacetime like phonons and the vibrations of the local oscillators, gains weight. Although experimentally an electron, a photon or a molecule released from a beable cannot be directly detected during the tiny burst, we can calculate the time development further with the time dependent Schrödinger equation. This is where in our theory we start a new time development: the electron is localized in a transient NIR on a carbonyl carbon atom in a single carbonyl CO fragment, the photon is in the protein cavity, no gravonons are involved.

During the tiny burst the exciton electron is no more entangled with the gravonons, it is released in a limbo state in $3D$ space, therefore cannot be directly accessed experimentally. But everything in the 2D spectroscopic experiment occurs during the tiny burst induced by the double laser pulse. This situation lasts until the entanglement with gravonons can develop again, giving rise to the beables. During the lifetime of the beable the exciton electron, which initially is a delocalized electron wave packet, remains localized transiently on the carbonyl carbon atom. Within this physical picture all measurable phenomena originate effectively from a very local region which then expands in $3D$ space. The chooser mechanism for the generation of the beables and the concept of the tiny burst due to the laser pulse indicate that what is measured in experiment has to be interpreted in a local picture concerning just a single carbonyl CO fragment in the protein backbone, which couples to no more than two local harmonic oscillators and the phonon excitations in the protein backbone. If more local harmonic oscillators were excited, which is possible only in the absence of the chooser mechanism, the result would be indeed fast decoherence of the photon beating signal. This is, however, not measured in experiment.

3 The Hamiltonian

The quantum fields in the model are: (i) electron; (ii) photon; (iii) gravonons; (iv) core movement field of the carbonyl CO fragment; (v) phonons. The total Hamiltonian, the gravonons taken into account as well, includes terms describing these fields and the many-particle interactions with the electron field:

$$H_{FMO} = H_{el} + H_{phot} + H_{grav} + H_{CO} + H_{phon} \\ + H_{el-phot} + H_{el-grav} + H_{el-CO} + H_{el-phon}. \quad (1)$$

The Hamiltonian for the electron includes single electron terms for exciton 1 within the chlorophyll assembly $|e\rangle$, exciton 2 in the chlorophyll assembly $|e'\rangle$, exciton 1 in the warp resonance $|w\rangle$, electron in the deformation resonance $|v\rangle$, electron in delocalized 'escape states' $\{|k\rangle\}$, the interaction of exciton 1 with the warp resonance and the interaction between the two excitons:

$$H_{el} = E_e c_e^\dagger c_e + E_{e'} c_{e'}^\dagger c_{e'} + E_w c_w^\dagger c_w + E_v c_v^\dagger c_v + \sum_k E_k c_k^\dagger c_k \\ + W_e (c_w^\dagger c_e + c_e^\dagger c_w) + W_{ee'} (c_e^\dagger c_{e'} + c_{e'}^\dagger c_e). \quad (2)$$

The Hamiltonian for the photon is:

$$H_{phot} = \omega_{phot} a^\dagger a \quad (3)$$

and for the non-perturbed gravonons:

$$H_{grav} = \sum_\kappa \varepsilon_\kappa \zeta_\kappa^\dagger \zeta_\kappa. \quad (4)$$

The Hamiltonian for the core movement of the carbonyl CO fragment in the deformation resonance (initial state and excited states) includes also the two local oscillators, describing the wagging and rocking motion of the carbonyl group, and their interaction:

$$H_{CO} = \epsilon_o d_o^\dagger d_o + E_d d^\dagger d + \sum_{i=1,2;n_i=0}^\infty n_i \omega_i d_{n_i}^\dagger d_{n_i} \\ + W_d \sum_{i=1,2;n_i=0}^\infty (d^\dagger d_{n_i} + d_{n_i}^\dagger d). \quad (5)$$

The Hamiltonian for the phonons is:

$$H_{phon} = \sum_p \omega_p b_p^\dagger b_p. \quad (6)$$

The many particle electron - photon interaction, giving rise to an exciton polariton, is described by the Hamiltonian:

$$H_{el-phot} = V_g (c_e^\dagger c_{e'} + c_{e'}^\dagger c_e) (a^\dagger + a) \quad (7)$$

and the many particle electron - gravonon interaction is described by the Hamiltonian:

$$H_{el-grav} = Y_w c_w^+ c_w \sum_{\kappa} (\zeta_{\kappa}^+ \zeta_o + \zeta_o^+ \zeta_{\kappa}). \quad (8)$$

The many particle interaction between the electron in the deformation resonance and the core movement of the carbonyl group includes interaction terms with the core movement states in the deformation resonance and in the local oscillators:

$$\begin{aligned} H_{el-CO} = & V_{core-def} (c_w^+ c_v + c_v^+ c_w) (d_o^+ d + d^+ d_o) \\ & + V_{core-loc} c_v^+ c_v \left(\sum_{i=1,2; n_i=0}^{\infty} d^+ d_{n_i} + \sum_{i=1,2; n_i=0}^{\infty} d_{n_i}^+ d \right), \end{aligned} \quad (9)$$

giving rise to the vibronic states. The many particle electron - phonon interactions are contained in the term:

$$H_{el-phon} = Y_p \sum_k (c_v^+ c_k + c_k^+ c_v) \sum_p (b_p^+ + b_p). \quad (10)$$

The meaning of the symbols in eqs. (2-10) is as follows:

$E_e, E_{e'}$ are single particle energies of exciton 1 and exciton 2 in the protein cavity and E_w, E_v, E_k denote the electron energy in the warp resonance $|w\rangle$ (localized at a single carbonyl carbon atom in one carbonyl CO fragment in the protein backbone), in the deformation resonance $|v\rangle$ and in the escape states $\{|k\rangle\}$. $c_e^+, c_e, c_{e'}^+, c_{e'}, c_w^+, c_w, c_v^+, c_v, c_k^+, c_k$ are the creation and destruction operators for the electron in the respective single electron states.

W_e is the interaction strength between exciton 1 and the warp resonance; $W_{ee'}$ is the interaction strength between exciton 1 and exciton 2.

ω_{phot}, a^+, a are used for the photon energy and photon creation and annihilation operators.

$\varepsilon_{\kappa}, \zeta_{\kappa}^+, \zeta_{\kappa}$ are the energy and creation and annihilation operators for the gravonons, which are treated in the quantum harmonic approximation. $\omega_{grav}(\beta^+ \beta + \frac{1}{2}) \equiv \sum_{\kappa} \varepsilon_{\kappa} \zeta_{\kappa}^+ \zeta_{\kappa}$ with $\varepsilon_{\kappa} = \omega_{grav}(n_{\kappa} + \frac{1}{2})$ is the parabola representation of the gravonons.

ϵ_o, d_o^+, d_o are used for the energy, the creation and annihilation operators for the initial core movement state $|d_o\rangle$ of the carbonyl CO fragment in the deformation resonance. E_d, d^+, d refer to the energy, creation and annihilation operators for the excited core movement state $|d\rangle$ of the carbonyl CO fragment in the deformation resonance.

n_i denotes the number of the energy level in the i -th local oscillator ($i = 1, 2$) with energy ω_i and creation and annihilation operators $d_{n_i}^+, d_{n_i}$ of vibrations in the n -th energy level of the i -th local oscillator.

W_d is the coupling strength between the vibrations of the carbonyl group CO in the deformation resonance and the local oscillators.

ω_p is the energy of the non-perturbed phonons in the protein backbone, with b_p^+, b_p the creation and annihilation operators for phonons in the protein backbone.

V_g is the electron-photon coupling strength in the cavity, creating the polariton.

Y_w is the coupling strength between the electron in the warp resonance $|w\rangle$ and the gravonons $\{| \kappa \rangle\}$.

With $V_{core-def}$ the interaction strength between the electron and the core movement state of the carbonyl group CO in the deformation resonance is denoted.

$V_{core-loc}$ is the interaction strength between the electron in the deformation resonance and the core movement states of the carbonyl group CO in the local oscillators.

Y_p refers to the coupling strength between the electron and the phonons $\{|p\rangle\}$ in the protein backbone.

The last term eq. (10) shows that when a phonon is excited in the protein backbone the electron has to decay from a local state in the deformation resonance in a delocalized electron escape state. This warrants the energy conservation required by Schrödinger's equation.

The second term in eq. (9) and the term in eq. (10) are responsible for the quantum beats, their exponential damping and the non-zero finite value of the photon signal produced by the stimulated electron deexcitation. The second term in H_{el-CO} (eq. 9) describes the interaction between the electron in the deformation resonance of the carbonyl CO fragment and the local oscillators. The term eq. (10) is the interaction of the electron with the delocalized phonons, excited in the protein backbone. The second interaction term in eq. (9) takes care of preserving the weight of local configurations with the electron involved and is responsible for the finite final amplitude of the photon signal, resulting from electron deexcitation, stimulated by the 3rd laser pulse. The interaction term eq. (10) takes care of the entanglement with the protein phonons. This is the dissipative term, which leads to the attenuation of the weight of electron configurations in the local region and causes the exponential damping of the amplitude of the stimulated photon emission signal with time.

The method of solving Schrödinger's equation for the time development of the total wave packet has been described in ref. (47). It uses a basis consisting of many particle configurations (the electron, the photon, gravonons, core movement of the carbonyl CO fragment, protein phonons) in a configuration interaction (CI) approximation. The local many particle basis includes notations for all fields (with gravonons and phonons in their initial states). For instance: $|e, 1, 0, 0, 0\rangle$, $|e', 0, 0, 0, 0\rangle$, $|w, 1, 0, 0, 0\rangle$, $|v, 1, 0, d, 0\rangle$, where in the first position the electron basis function is denoted, in the second place the photon state, in the third place: the gravonon state, in the fourth place: core movement state of the carbonyl CO fragment and in the fifth place: the protein backbone phonon state.

The specific feature of the theoretical approach applying to the green sulfur bacteria is the choice of the matrix elements. The energy difference between exciton 1 and exciton 2 equals 22 meV and is of the order of magnitude determined experimentally (55) and used in other approaches (56). For the interaction matrix element between the two excitons we use 20 meV, and 12 meV for the coupling between the exciton and the warp resonance.

After diagonalizing to first order in the basis the time dependent Schrödinger equation is solved:

$$|\Psi(t)\rangle = e^{-iH_{FMO}t} |\Psi(0)\rangle. \quad (11)$$

As described in section 2 we solve the TDSE twice. In the first calculation the initial state $|\Psi(0)\rangle$ is an extended exciton state which develops into a localized beable. In the second calculation the initial state $|\Psi(0)\rangle$ has the exciton electron in the beable state (3s-affinity orbital of the carbonyl carbon atom) as described in section 2.

The single particle basis states are:

- (i) the electron in the excitons $|e\rangle$, $|e'\rangle$ and in the warp resonance $|w\rangle$, in the deformation resonance $|v\rangle$ and in the escape states $\{|k\rangle\}$;
- (ii) the photon: 1: with photon in the protein cavity, 0: no photon;
- (iii) gravonons: 0: for initial state of the gravonon continuum, $\{\kappa\}$ for excited gravonons;
- (iv) the carbonyl CO group in its vibrational state in the deformation resonance: (0 for initial vibrational state; d in an excited vibrational state) and the carbonyl CO group in the wagging or rocking vibrational state, described by the local oscillators (ω_i is the energy of the i -th local oscillator in its n -th state $|d_{ni}\rangle$);
- (v) the protein backbone phonon state: 0 for protein phonons in their initial state, $\{p\}$ for excited protein phonons.

3.1 Vibrational energy in the local oscillators

An estimate of the vibrational excitation energy of the rocking and wagging motions of the carbonyl group in the protein backbone of the order of $\omega \approx 5$ meV is based on the experimental data in ref. (2). With this estimate at thermal energy of approximately $k_B T = 11$ meV at $T = 125$ K two local vibrations can be excited each with $\omega_1 = \omega_2 = \omega \approx 5$ meV, so that $2\omega \approx 10$ meV corresponds approximately to the thermal energy at 125 K. The rocking and wagging motions of the carbonyl group are much softer than its vibration with respect to the protein chain, hence 5 meV for the quantum of these vibrations appears physically plausible.

The energy of a local vibration can be neither 4 meV nor 6 meV because these values contradict the experimental curves for 77 K, 125 K and 150 K. The estimate for the energy of the local mode $\omega \approx 5$ meV, based on the 2D Fourier transform spectroscopy experiment, corresponds to the thermal energy $k_B T$ at $T \approx 58$ K. At $T = 125$ K and $T = 150$ K the two experimental curves coincide. If by $T = 125$ K two quanta are excited, then at $T = 150$ K it is not possible to excite 3 quanta, hence 2 excited quanta would explain the coinciding curves in experiment. The two quanta 2ω should correspond to $T = 125$ K and $k_B T \approx 11$ meV, hence $\omega \approx 5$ meV. ω cannot be 4 meV ($T \approx 46$ K) because then at $T = 150$ K three vibrational quanta will be excited, whereas at $T = 125$ K only two can be excited and the two curves will not coincide. ω cannot be 6 meV ($T \approx 70$ K) either because at $T = 125$ K, $k_B T \approx 11$ meV, just a single local vibration will be excited exactly as by $T = 77$ K. The two curves at $T = 77$ K and $T = 125$ K would coincide. This is, however, not observed experimentally.

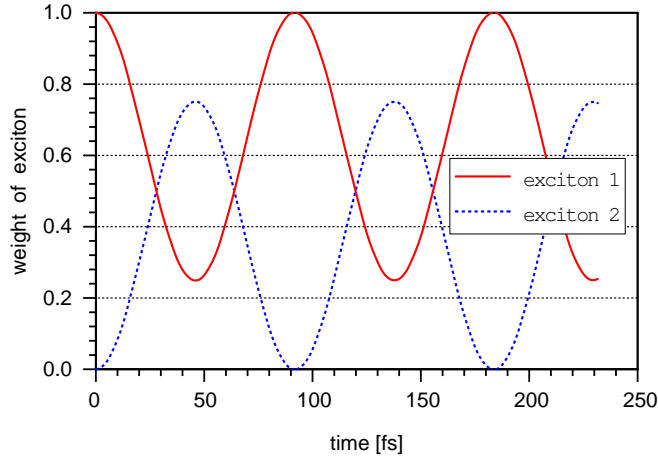


Figure 3: Rabi oscillations between the two exciton states isolated from the environment.

3.2 Protein phonon band

The protein phonon band width is of the order of 0.03 eV. This follows from the following argument. Assume a periodic constant of a simple one dimensional protein of the order of $a \approx 10$ bohr, then the maximal wave vector k_{max} is of the order of $k_{max} = \frac{\pi}{a} \approx 0.3 \text{ bohr}^{-1}$. The energy corresponding to the maximal k -vector is $\omega_{p,max} = v k_{max} = 0.027 \text{ eV}$ (using for the sound velocity in dry air $v = 330 \text{ m/s} = 6.6 \times 10^{12} \text{ bohr/s}$). This estimate refers to the transversal phonon modes.

4 Results for the time development of the tiny burst

We assume that the exciton electron is in a beable before the laser pulses occur, because the bacterium exists in reality and therefore cannot be in a limbo state. Reality consists of beables only.

The results of the calculation leading to the beable have been presented in fig. 2. We now discuss what happens after the beable has been destroyed by the laser pulse.

The first laser pulse in the 2D spectroscopic experiment excites the FMO complex electronically producing the first exciton delocalized in the protein cavity. The second laser pulse excites the second exciton and a coherent superposition between the two (57). If no interaction with the environment exists the coherent oscillations between exciton 1 and exciton 2 will continue, the amplitude of each state changing sinusoidally with time (fig. 3).

However, for the FMO-protein complex we have the protein cavity and the chlorophyll molecules within the cavity. Before the tiny burst the exciton electron is transiently localized in a single warp resonance on a carbon atom at a single carbonyl CO fragment chosen by degeneracy

with the gravonons. The photon is in the cavity. The localized electron exercises a force on the carbon atom, exciting two local oscillators with the wagging and rocking movements of the carbonyl CO fragment in the deformation resonance. In addition to coupling to the local oscillators, coupling to the extended protein phonons within the deformation resonance allows relaxation and dissipation in delocalized phonons away from the local site. In the 2D Fourier transform electronic spectroscopy experiments these components are not observed, the measurement provides just the amplitude of the photon echo, which scales with the weight of the local configurations involving the exciton electron, as a function of time. But we can calculate the time development of the wave packet during the period of the tiny burst and it shows a strong similarity with the variations with time of the photon amplitude measured experimentally (fig. 4).

In experiment the third laser pulse after a waiting time T stimulates the photon emission. At time T the photon is emitted with the amplitude, with which the electron to be deexcited is represented in the local components of the wave packet (warp resonance, deformation resonance, local oscillators) just before the third laser pulse. Our theory ends at the moment just before the third laser pulse is shot. The third laser pulse will cause stimulated photon emission with the amplitude, with which the exciton electron is represented in all configurations involving the local states: the warp resonance, the deformation resonance and the local oscillators. The sum of the squared amplitudes of these configurations is plotted as a function of time in fig. 4. The amplitude of the emitted photon signal scales with the weight of all local configurations involving the exciton electron. In experiment choosing the photon in the detector via a new beable happens with an amplitude equal to the sum of the squared coefficients of those configurations, which have the exciton electron, whose deexcitation is stimulated by the third laser pulse.

4.1 Temperature effects

For the solution of the time dependent Schrödinger equation at different temperatures we explicitly need the dependence of the accessible vibrational configurations on temperature, i.e. counting of the vibrational configurations in the deformation resonance, and the temperature dependence of the accessible on-shell phonon configurations. The assumption is that the deformation resonance is as highly excited as the external temperature allows. This energy can then be redistributed between the local channels and the delocalized phonons.

We assume that within the deformation resonance coupling to two local quantum harmonic oscillators is effective, associated with the rocking and wagging motions of the carbonyl CO fragment. Einstein's model is assumed (non-interacting oscillators with the same frequency). One local oscillator is not enough to reproduce the temperature dependence of the signal, it is not able to compete with the dissipative effect of the protein phonons. If it were just one local harmonic oscillator available for relaxation (one relaxed vibrational mode) we would get fast decay of the photon amplitude and no temperature dependence since one oscillator provides one local vibrational configuration for all experimental temperatures. If the number of coupled local oscillators and local vibrational configurations were large, i.e. the exciton elec-

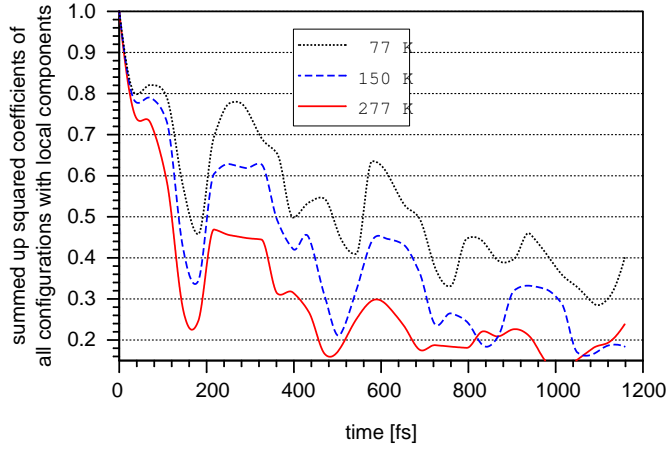


Figure 4: Time development of the amplitude of the photon signal during the tiny burst, induced by the double laser pulse, for the model in fig. 1 at three different temperatures of the environment. The photon signal scales with the summed weight of the field configurations with local components in the wave packet. These are configurations with the exciton electron in the warp resonance (i.e. in the beable), in the deformation resonance and the local oscillators. The initial state is the beable described in the text.

tron resides transiently on many carbonyl carbon atoms in many carbonyl CO fragments, we would get no temperature dependence of the decay of the photon amplitude either. It would immediately drop to zero as decoherence theory suggests. No chooser effect and fast decay in the protein phonons all over the protein chain would be the result. This is a situation when the local structure is lost. Hence, the result would be fast exponential decay of the photon signal as anticipated by decoherence theory. However, in our model, starting from a delocalized exciton electron, with the chooser mechanism due to on-shell entanglement with gravonons, a localized electron in the form of a beable is generated. The local nature of the interactions in this many particle system prevents the excitation of many harmonic oscillators over the protein chain and the total decay of the photon signal.

With two local oscillators we get the exponential damping of the photon amplitude with time, the beating of the photon signal and the finite non-zero value of the photon signal at long time as shown in fig. 4. The temperature dependence is also in satisfactory agreement with the experimental observation.

The dependence of the photon signal on the temperature is reflected by changes in the vibrational structure of the local oscillators and the accessibility of the protein phonon configurations. The temperature dependence of the accessible vibrational configurations due to the local oscillators and the delocalized phonon configurations in the protein is treated in the following way. Figure 5 illustrates how the local oscillator vibrational structure changes with temperature if we restrict the model to two local oscillators. The wagging and the rocking modes are assumed to have the same energy $\omega = 5$ meV. This energy corresponds roughly

to thermal energy $k_B T$ at $T = 58$ K. The energy is provided by the external heating and is available within the deformation resonance. So if the temperature in the 2D Fourier transform spectroscopy experiment equals 77 K, it means that either one or the other local oscillator can be excited, i.e. there are two degenerate vibrational configurations due to the local oscillators involved in the interaction with the deformation resonance (the first line in fig. 5). At $T = 125$ K and $T = 150$ K the available thermal energy is sufficient to excite just 2 local vibrations which makes three degenerate local vibrational configurations (the second line in fig. 5) and so on. Thus, when the temperature rises the local vibrational structure becomes more complex. As the temperature rises 2, 3, 4 ... local vibrational configurations, which are energetically accessible and are on the energy shell with respect to the energy of the exciton wave packet, will be involved. More and more on-shell local channels get open for the wave packet when the temperature rises. This is the decisive feature of the model, which prevents the destruction of the coherent time development by decoherence and the total decay in the protein phonons.

Because we solve Schrödinger's equation with a procedure similar to CI, we see that the number of the configurations involved increases with the increasing energy, i.e. with increasing temperature.

The channels for decay in delocalized protein phonons also increase, the available density of phonon configurations on the energy shell of the initial wave packet increases linearly with temperature. This is so because we assume a one-dimensional protein chain with constant density of states which provides a linear dependence on the temperature of the on-shell density of phonon configurations. If we would take the 3D Debye model for the phonons the density of on-shell phonon configurations would vary with T^3 , which would result in fast dissipation in phonons, accompanied by the decay of the electron in the delocalized escape states.

The higher the temperature, the more protein phonon configurations are accessible on the energy shell. Assume the energy in the deformation resonance is 11 meV corresponding to a temperature of 125 K. The phonon configurations in the protein backbone which preserve the energy of the total wave packet can vary their energy upto 11 meV. Assume now that the energy in the deformation resonance is 22 meV corresponding to 250K. The number of phonon configurations, which can preserve the total energy of the wave packet and thus leave it on the energy shell, is much larger.

The two channels, governed by the terms in the Hamiltonian:

$$H_{el-CO} = \dots + V_{core-loc} c_v^\dagger c_v \left(\sum_{i=1,2;n_i=0}^{\infty} d^\dagger d_{n_i} + \sum_{i=1,2;n_i=0}^{\infty} d_{n_i}^\dagger d \right)$$

and

$$H_{el-phon} = Y_p \sum_k (c_v^\dagger c_k + c_k^\dagger c_v) \sum_p (b_p^\dagger + b_p)$$

compete. The first term has the effect of conserving the amplitude of the wave packet in the local region, whereas the second leads to its decay out of the local region in the delocalized

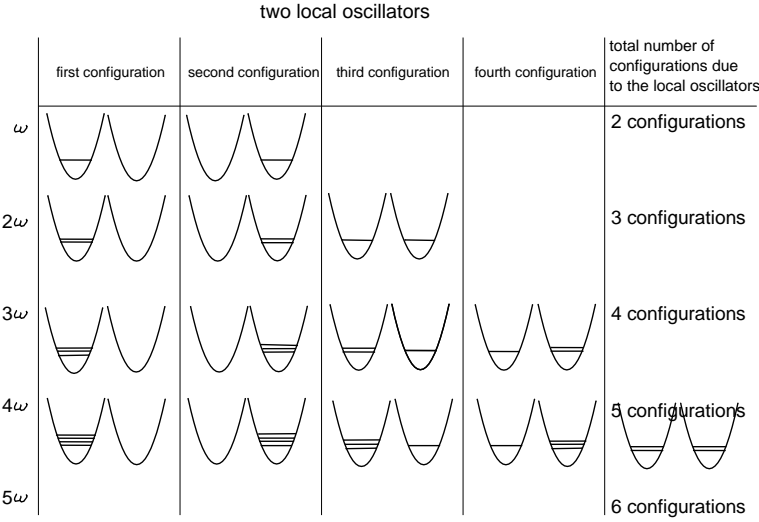


Figure 5: Local vibrational configurations on the energy shell of the initial wave packet as a function of the excitation energy, hence as a function of the temperature, available within the deformation resonance.

protein phonons, which are not measured in the experiment, causing the exponential damping of the photon signal at short time. As time goes by the two competing effects balance each other and the photon signal gets stabilized at a finite value.

As the local structure in the model comprises more and more configurations with rising temperature it has a counterbalancing effect on the decay due to coupling to the delocalized phonons and warrants that the weight of local configurations with the exciton electron is retained locally. Then the third laser pulse in the experiment can interact with the localized electron in the $3s$, the deformation resonance and the local oscillators and stimulate the photon emission with the amplitude retained in the local structure.

For our result the localized initial beable state is decisive. In our theory we start from a local beable and follow its time development during the tiny burst. Since the local structure expands in number of configurations with rising temperature, the wave packet does not delocalize completely and remains local. This reminds qualitatively of the quantum Zeno effect, which is collapse after each interaction event with the environment. However, the time development of the total system in high dimensional space is completely coherent. The stochastic approaches try to obtain similar effects by an empirical special choice and tuning of the phonon noise such that the experimental beating signal is reproduced (32).

5 Discussion

As we see that with the simple model we reproduce the experimental dependence of the photon amplitude on the waiting time and the temperature, which is observed in the 2D Fourier transform electronic spectroscopy, we can suggest an explanation of the questions raised in the introduction.

No isotope effect on the coherences in FMO is established experimentally. In our theory it is of no significance if 1H is replaced by 2H or ^{12}C is exchanged with ^{13}C . The local vibrational spectrum changes, but we only need the spectrum on the energy shell of the wave packet. The local picture explains why if something changes 10 Å away from the transient negative ion resonance, for instance isotopes of hydrogen are exchanged, the change does not affect the coherent behaviour of the NIR, which is observed in experiment.

Using an argument from perturbation theory, the first order coupling between two configurations scales with the inverse of their energy difference. The closer the energy of the interacting configurations, the stronger the interaction between them and the first order term will provide the major contribution. Hence, the on-shell contribution to the coupling dominates. Therefore the many particle configurations we take into account, are nearly on-shell with the initial wave packet since they provide the major contributions to the coupling.

Reminding the many-particle character of the field configurations in our theory we necessarily have to conclude that the nature of the states involved in the superposition, leading to the quantum beats, is vibronic, as it has been suggested by experimentalists as well.

Why does conventional decoherence not prevail? The initial state in a conventional decoherence approach is the superposition of exciton states delocalized over the protein cavity. The environment are the protein phonons, the coupling of the excitons with the environment leads to phonon excitation. Energy conservation requires that the excitons are deexcited in the ground electron state. No oscillations between the electron ground and exciton states can occur. With the argument used by decoherence theory, the reduced density matrix has then a single non-zero diagonal matrix element equal to 1 for the electron ground state of the excitons.

This would happen if we would neglect the chooser mechanism, which localizes the electron in the $3s$ -affinity orbital of the carbonyl carbon atom. In an attempt to simulate the result of decoherence theory let us omit the local oscillators due to the carbonyl CO fragment, as in decoherence theory they play no role. The initial state is also changed, the electron is no more 'chosen' in the warp resonance, it is assumed to be in the somewhat diffuser deformation resonance. If in our model we would disregard the chooser mechanism and the coupling to the local CO oscillators and allow the exciton electron to couple to phonon continua all over the protein chain the result is similar to what is expected from decoherence theory (fig. 6). The two curves in fig. 6 are evaluated with different initial states, of course. Whereas for the upper curve the exciton electron in the initial wave packet is localized via the chooser mech-

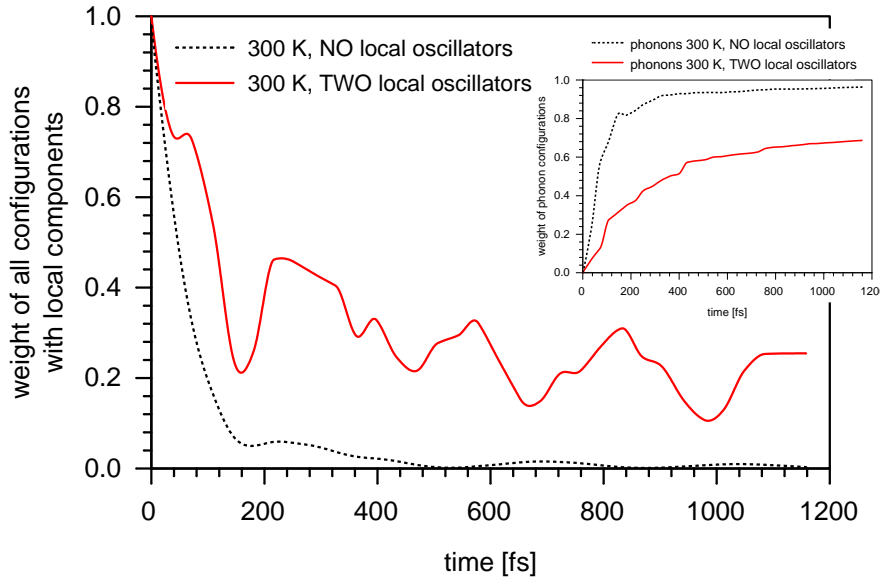


Figure 6: Time development of the photon amplitude in a model neglecting the coupling of the exciton electron to the local oscillators with dominating coupling to the phonons (decaying dashed curve), corresponding to temperature 300 K, compared to the result with the local structure included (oscillating full curve). Inset: development with time of the weight of field configurations involving the protein phonons with the local structure included (full curve) and excluded (dashed curve).

anism in the beable, for the lower curve where no chooser mechanism is operating, the initial wave packet has the electron in the deformation resonance. Ignoring the chooser mechanism leads to an exponential decay of the photon amplitude without oscillations to zero value, completely and irreversibly. Everything is lost in the protein phonons (cf. the dashed curve in the inset in fig. 6), and this is not measured in the experiment. This resembles the prediction of conventional decoherence theory. In contrast, the chooser mechanism due to degeneracy entanglement with gravonons determines the transient localization of the electron wave packet in a beable and precludes its total decay in the environmental phonon continuum, which is the reason for retaining finite photon amplitude for long time, at least within the lifetime of the tiny burst.

The curve, which reproduces the experimental result, starts with the exciton electron in a beable (which is destroyed by the photon-induced tiny burst) localized in the NIR via the chooser mechanism due to entanglement with the gravonons. The exponentially decaying photon amplitude curve is evaluated by neglecting the chooser mechanism, the electron is in the deformation resonance, where it couples with the dissipative phonon environment all over the protein backbone.

The role of the gravonons, although they are not involved during the time of the tiny burst, is to create the beable via the chooser mechanism. The transient trapping of the exciton elec-

tron in the $3s$ -affinity orbital on the carbonyl carbon atom due to the entanglement with the degenerate gravonons occurs before the double laser pulse and the tiny burst. The laser pulse generates the tiny burst and causes the bursting of the $3D$ components of the total wave packet in $3D$ space and the destruction of the entanglement with the gravonons (cf. fig. 2 and the inset showing how $3D$ components of the wave packet gain weight during the tiny burst).

From our theory and the measurements it appears that **decoherence is an illusion**. If it did exist it would have led to the total decay of the photon signal within femtoseconds, as the decaying dashed curve in fig. 6 shows. Some obvious arguments can be summarized:

(i) Despite that in the present theory standard decoherence theory due to coupling to environmental degrees of freedom is **not** involved, all experimental observations are reproduced in a coherent picture by solving the TDSE. Reduced density operator and matrix, being the basis for the conclusions in decoherence theory, are neither needed nor used. The chooser mechanism localizes the exciton electron within the beable, allowing it to interact with the local core movement states of the carbonyl group in addition to the dissipative interaction with the phonons in the protein backbone. In our theory these are physical phenomena within a completely coherent picture.

(ii) Decoherence theory misses the localization in a beable. It starts from an initial state with a delocalized exciton electron. In contrast, in the present theory we reproduce and explain the experiments on the coherent behaviour of the protein-FMO complex as effects of the local structure and its temperature dependence. The generation of a local beable via entanglement of the exciton electron with gravonons is the clue to the understanding of the experiment. In contrast, decoherence theory has no local beables, therefore it cannot provide the explanation of the long-living coherence of FMO.

(iii) In the stochastic approaches, based on the reduced density matrix and hence decoherence, special constructions of environmental excitations, in particular special phonons (colour-noise), are suggested as a decohering environment to be able to reproduce the experimental curves. Arguments are suggested concerning the efficiency of electron transfer from the FMO complex to the reaction center. But experiment shows the coherent behaviour and **no** dependence of the coherent behaviour on the protein phonon structure.

(iv) Stochastic approaches, missing localization in beables, cannot provide an explanation of the non-zero value of the photon echo amplitude at long time. No explanation is suggested why should the phonons not be able to reduce the photon echo amplitude to zero. If decoherence were active, the large number of environmental degrees of freedom involved should lead to complete decay of the photon echo signal.

6 Conclusion

We can understand the experimental results of long time coherence in the FMO protein complex without the far-fetched assumption of special phonons involved in the approach based on stochastic quantum master equations. Our understanding is based on the localization of the exciton electron due to a localization chooser mechanism using gravitation in high dimensional spacetime. Released from the entanglement with the gravonons by the laser pulses,

the electron can couple with local vibrations of the carbonyl CO group and the delocalized phonons in the protein backbone. This determines the vibronic character of the many-particle configurations leading to the beating of the photon echo signal. The two channels lead to preservation of a local non-vanishing weight of the exciton electron and to the beating photon echo signal and its exponential damping. Conventional decoherence theory would in fact predict a total exponential decay of the signal and much faster total loss of coherence compared to the experimentally established coherence times.

In order to understand the finite final value of the photon echo signal in 2D Fourier transform electronic spectroscopy at long time we involve a very local structure and then a temperature dependent accessibility to the local structure. The starting point in our theory on the coherent behaviour of chlorophyll assemblies is the localized exciton electron as a beable which allows the interaction of this localized charge with the photon field. The further time development of the wave packet follows from the initial localization of the electron.

The stepwise bunching of photon-amplitude curves at different temperatures (fig. 3 for $T = 125$ K and $T = 150$ K in ref. (2)) is only possible if we have a local picture with excitation of only a few local oscillators. This point needs to be further investigated experimentally since the error bars in the experimental figure in ref. (2) are larger than the expected differences between the curves.

The observation that isotope substitution does not change the experimentally measured photon echo amplitude is explained in our theory. No special phonons ('colour noise', special spectral function) are needed to explain the coherent behaviour and the damped amplitude of the photon beating signal with time.

We explain the magic non-appearance of decoherence in the 2D Fourier transform electronic spectroscopic experiment.

To finalize, we claim that quantum mechanics needs a chooser mechanism for particle localization. Experiments can be explained within quantum mechanics only if the incoming delocalized particle wave gets localized on a local site. The solution of the time dependent Schrödinger equation in high dimensional spacetime including the entanglement to gravonons is the theory of the chooser mechanism.

Local beables are the fundament of measurement. The measurement gives data on local features and this is what Schrödinger's equation with entanglement with the gravonons in high dimensional spacetime ($11D$) provides. All measured particles are local, they are local only when they entangle with gravonons as beables.

Acknowledgment: We gratefully acknowledge the useful discussion and comments by G. Engel at the Gordon Center for Integrative Science, Chicago University.

References

- [1] G.S. Engel, T.R. Calhoun, E.L. Read, T. Ahn, T. Manc  l, Y. Cheng, R.E. Blankenship and G.R. Fleming, *Nature* **446**, 782 (2007).
- [2] G. Panitchayangkoon, D. Hayes, K.A. Fransted, J.R. Caram, E. Harel, J. Wen, R.E. Blankenship and G.S. Engel, *Proc. Nat. Acad. Sci. USA* **107**, 12766 (2010)
- [3] G. Panitchayangkoon, D.V. Voronine, D. Abramavicius, J.R. Caram, N.H.C. Lewis, S. Mukamel and G.S. Engel, *Proc. Nat. Acad. Sci. USA* **108**, 20908 (2011).
- [4] M.W. Johnson et al. *Nature* **473**, 194 (2011).
- [5] N.G. Dickson et al. *Nature Communications* 4:1903, DOI: 10.1038/ncomms2920, 2013.
- [6] D. Drakova and G. Doyen, arxiv:1220200 [quant-ph] 31 Mar 2015.
- [7] D. Drakova and G. Doyen, *J. Phys.: Conf. Series* **442**, 012049 (2015).
- [8] P. Rebentrost, M. Mohseni and A. Aspuru-Guzik, *J. Phys. Chem. B* **113**, 9942 (2009).
- [9] M. Mohseni, A. Aspuru-Guzik, P. Rebentrost, A. Shabani, S. Lloyd, S.F. Huelga and M.B. Plenio, in: *Quantum effects in biology*, Eds. M. Mohseni, Y. Omar, G.S. Engel and M.B. Plenio, Cambridge Univ. Press 2014, p. 159.
- [10] G.S. Engel, in: *Quantum effects in biology*, Eds. M. Mohseni, Y. Omar, G.S. Engel and M.B. Plenio, Cambridge Univ. Press 2014, p. 144.
- [11] J. Al-Khalili and J. McFadden, *Life on the edge - The coming of age of quantum biology*, Bantam Press, 2014.
- [12] H. Lee, Y.-C. Cheng and G.R. Fleming, *Science* **316**, 1462 (2007).
- [13] V.P. Singh, M. Westberg, C. Wang, P.D. Dahlberg, T. Gellen, A.T. Gardiner, R.J. Cogdell and G.S. Engel, *J. Chem. Phys.* **142**, 212446 (2015).
- [14] E. Harel and G.S. Engel, *Proc. Natl. Acad. Sci. U.S.A.* **109**, 706 (2012).
- [15] A.F. Fidler, V.P. Singh, P.D. Long, P.D. Dahlberg and G.S. Engel, *J. Phys. Chem. Lett.* **4**, 1404 (2013).
- [16] E. Collini, C.Y. Wang, K.E. Wilk, P.M. Curmi, P. Brumer and G.D. Scholes, *Nature* **463**, 644 (2010).
- [17] P.D. Dahlberg, A.F. Fidler, J.R. Caram, P.D. Long and G.S. Engel, *J. Phys. Chem. Lett.* **4**, 3636 (2013).
- [18] P.D. Dahlberg, G.J. Norris, C. Wang, S. Viswanathan, V.P. Singh and G.S. Engel, *J. Chem. Phys.* **143**, 101101 (2015).

- [19] P. Rebentrost, M. Mohseni, I. Kassal, S. Lloyd and A. Aspuro-Guzik, New J. Phys. **11**, 033003 (2009).
- [20] M. Mohseni, P. Rebentrost, S. Lloyd and A. Aspuro-Guzik, J. Chem. Phys. **129**, 174106 (2008).
- [21] A. Ishizaki and G.R. Fleming, Proc. Natl. Acad. Sci. U.S.A., **106**, 17255 (2009).
- [22] R. Hildner, D. Brinks and N.F. van Hulst, Nature Physics **7**, 172 (2011).
- [23] I. Chiorescu, Y. Nakamura, C.J.P.M. Harmans and J.E. Mooij, Science **299**, 1869 (2003).
- [24] J.D. Hybl, A.A. Ferro and D.M. Jonas, J. Chem. Phys. **115**, 6606 (2001).
- [25] M.L. Cowan, J.P. Ogilvie, R.J.D. Miller, Chem. Phys. Lett. **386**, 184 (2004).
- [26] T. Brixner, T. Mančal, I.V. Stiopkin and G.R. Fleming, J. Chem. Phys. **121**, 4221 (2004).
- [27] D. Abramavicius, D.V. Voronone and S. Mukamel, Biophys. J. **94**, 3613 (2008).
- [28] A. Nagy, V. Prokhorenko and R.J.D. Miller, Curr. Opin. Struct. Biol. **16**, 654 (2006).
- [29] O.V. Prezhdo and P.J. Rossky, Phys. Rev. Lett. **81**, 5294 (1998).
- [30] E. Joos and H.D. Zeh, J. Phys. Cond. Matter **59**, 223 (1985); E. Joos, H.D. Zeh, Z. Phys. B: Cond. Matter, **59**, 223-243 (1985).
- [31] W.H. Zurek, Phys. Rev. D **24**, 1516 (1981); Rev. Mod. Phys. **75**, 715 (2003).
- [32] A. Shabani, M. Mohseni, S. Yang, A. Ishizaki, M. Plenio, P. Rebentrost, A. Aspuro-Guzik, J. Cao, S. Lloyd and R. Silbey, in *Quantum effects in biology*, eds. M. Mohseni, Y. Omar, G. Engel and M.B. Plenio, Cambridge University Press, 2014, p. 14.
- [33] T. Förster, Naturwissenschaften **33**, 166 (1946); T. Förster, Ann. Physik **437**, 55 (1948);
- [34] R.A. Marcus and N. Surin, Biochem. Biophys. Acta **811**, 265 (1985).
- [35] J.J. Hopfield, Proc. Natl. Acad. Sci. USA **9**, 3640 (1974).
- [36] D. Dester, J. Chem. Phys. **21**, 836 (1953).
- [37] M. Şener, J. Strümpfer, J. Hsin, D. Chandler, S. Sheuring, C.N. Hunter and K. Schulten, Chem. Phys. Chem. **12**, 518 (2011).
- [38] A. Chenu and G.D. Scholes, Annu. Rev. Phys. Chem. **66**, 69 (2015).
- [39] V. Tiwari, W.K. Peters and D.M. Jonas, Nat. Chemistry **6**, 173 (2014).
- [40] F.D. Fuller, J. Pan, A. Gelzinis, V. Butkus, S.S. Senlik, D.E. Wilcox, C.F. Yocum, L. Valkunas, D. Abramavicius and J.P. Ogilvie, Nat. Chemistry **6**, 706 (2014).

- [41] E. Romero, R. Augulis, V.I. Novoderezhkin, M. Ferretti, J. Thieme, D. Zigmantas and R. van Grodelle, *Nat. Physics* **10**, 677 (2014).
- [42] E. Romero, V.I. Novoderezhkin and R. van Grodelle, in: *Quantum effects in biology*, Eds. M. Mohseni, Y. Omar, G.S. Engel and M.B. Plenio, Cambridge Univ. Press 2014, p. 179.
- [43] A. Chenu, N. Christensson, H.F. Kauffmann and T. Manc l, *Sci. Rep.* **3**, 2029 (2013).
- [44] J.M. Womick and A.M. Moran, *J. Phys. Chem. B* **115**, 1347 (2011).
- [45] D. Hayes, J. Wen, G. Panitchayangkoon, R.E. Blankenship and G.S. Engel, *Faraday Discuss.* **150**, 459 (2011).
- [46] G.S. Schlau-Cohen, A. Ishizaki, T.R. Calhoun, N.S. Ginsberg, M. Ballottari, R. Bassi and G.R. Fleming, *Nat. Chemistry* **4**, 389 (2012).
- [47] G. Doyen and D. Drakova, *Found. Phys.* **45**, 959 (2015).
- [48] J.S. Bell, *Speakable and Unsayable in Quantum Mechanics: The theory of local beables*, Cambridge U.P. 2004, 2nd edition, p. 52.
- [49] A.J. Dempster, H.F. Batho, *Phys. Rev.* **30**, 644 (1927).
- [50] V.B. Braginski, F.Y. Khalili, *Quantum Measurement*, Cambridge U.P. 1992, p 3.
- [51] L. Hackerm ller, S. Uttenthaler, K. Hornberger, E. Reiger, B. Brezger, A. Zeilinger, M. Arndt, *Phys. Rev. Lett.* **91**, 090408 (2003).
- [52] K. Hornberger, S. Gerlich, Ph. Haslinger, S. Nimmrichter, M. Arndt, *Rev. Mod. Phys.* **84**, 157 (2012).
- [53] Th. Juffmann, A. Milic, M. M llneritsch, P. Asenbaum, A. Tsukernik, J. T xen, M. Mayor, O. Cheshnovsky, M. Arndt, *Nature Nanotech.* **7**, 297 (2012).
- [54] G. Doyen and D. Drakova, *J. Phys.: Conf. Series* **442**, 012063 (2015).
- [55] J.R. Caram and G.S. Engel, *Faraday Discuss.* **153**, 93 (2011).
- [56] A. Ishizaki and G.R. Fleming, *J. Chem. Phys.* **130**, 234111 (2009); *Ann. Rev. Condens. Matter Phys.* **3**, 333 (2012)
- [57] G.R. Fleming, M. Yang, R. Agarwal, B.S. Prall, L.J. Kaufman and F. Neuwahl, *Bull. Korean Chem. Soc.* **24** (8), 1081 (2003).
- [58] H. Ollivier and W.H. Zurek, *Phys. Rev. Lett.* **88**, 017901 (2002).